AIP | Journal of Applied Physics

Thermoelectric power factors of nanocarbon ensembles as a function of temperature

D. M. Gruen, P. Bruno, R. Arenal, J. Routbort, D. Singh et al.

Citation: J. Appl. Phys. **105**, 073710 (2009); doi: 10.1063/1.3103244
View online: http://dx.doi.org/10.1063/1.3103244
View Table of Contents: http://jap.aip.org/resource/1/JAPIAU/v105/i7
Published by the American Institute of Physics.

Thermoelectric power factors of nanocarbon ensembles as a function of temperature

D. M. Gruen,[1,a)] P. Bruno,[1] R. Arenal,[1,2] J. Routbort,[3] D. Singh,[4] and M. Xie[1,5]
[1]*Materials Science Division, Argonne National Laboratory, Argonne, Illinois 60439, USA*
[2]*Laboratoire d' Etude des Microstructures, CNRS-ONERA, BP 72 92322 Chatillon, France*
[3]*Energy System Division, Argonne National Laboratory, Argonne, Illinois 60439, USA*
[4]*Nuclear Engineering Division, Argonne National Laboratory, Argonne, IL 60439, USA*
[5]*Department of Physics, Michigan Technological University, Houghton, MI 49931, USA*

(Received 2 February 2009; accepted 16 February 2009; published online 13 April 2009)

Thermoelectric power factors of nanocarbon ensembles have been determined as a function of temperature from 400 to 1200 K. The ensembles, composed of mixtures of nanographite or disperse ultrananocrystalline diamond with B_4C, are formed into mechanically rigid compacts by reaction at 1200 K with methane gas and subsequently annealed in an argon atmosphere at temperatures up to 2500 K. The ensembles were characterized using scanning electron microscopy, Raman, x-ray diffraction, and high resolution transmission electron microscopy techniques and found to undergo profound nanostructural changes as a function of temperature while largely preserving their nanometer sizes. The power factors increase strongly both as a function of annealing temperature and of the temperature at which the measurements are carried out reaching 1 $\mu W/K^2$ cm at 1200 K without showing evidence of a plateau. Density functional "molecular analog" calculations on systems based on stacked graphene sheets show that boron substitutional doping results in a lowering of the Fermi level and the creation of a large number of hole states within thermal energies of the Fermi level [P. C. Redfern, D. M. Greun, and L. A. Curtiss, Chem. Phys. Lett. 471, 264 (2009)]. We propose that enhancement of electronic configurational entropy due to the large number of boron configurations in the graphite lattice contributes to the observed thermoelectric properties of the ensembles. © *2009 American Institute of Physics*. [DOI: 10.1063/1.3103244]

I. INTRODUCTION

Thermoelectrics are unique in that they convert heat to electricity directly using solid-state technology, thus avoiding pressurized fluids and rotating machinery. Devices based on this approach to energy conversion have operated successfully and reliably providing power for space vehicles without requiring maintenance even during decade-long missions. Conversion efficiencies typical of current thermoelectrics are of the order of 10%. The mounting pressures on energy resources have understandably led to an intense worldwide effort to achieve increases in efficiency which if substantial enough would enable thermoelectric conversion to compete with electromagnetic induction technologies. Although there appear to be no fundamental reasons why this cannot be done, major materials development challenges must be overcome to reach this elusive goal.[1] The ongoing quest has centered in recent years on the development of a variety of different ways in which certain desirable properties of nanomaterials can be utilized to increase thermoelectric performance.[2] The phonon-glass electron-crystal paradigm appears to apply particularly well to nanomaterials where phonon scattering at the ubiquitous grain boundaries leads to large decreases in the thermal conductivity compared to bulk materials.[3] Again, the reduced dimensionality of nanomaterials can strongly influence the electronic structures of the valence or conduction bands very near the Fermi level, for example, by increasing the density of states, thus enhancing the thermopower or Seebeck coefficient. Employing these concepts, remarkable progress has, in fact, allowed the figure of merit, *ZT*, to reach values in excess of 2 in the case of superlattices or quantum dots. Such structures, however, are in general not stable at the temperatures at which power generating devices would have to operate. Thermoelectrics are heat engines and their conversion efficiencies are strongly dependent on the magnitude of the temperature differentials between hot and cold junctions. To take advantage of this fact, one wants to operate the hot junction continuously at temperatures of about 1400 K. Very few materials preserve their nanocrystallinity under such conditions. It is for this reason that carbon and, in particular, boron doped nanocarbons were chosen as model systems for studies of their thermoelectric performance characteristics.[4]

In that earlier work it was shown that reaction of disperse ultrananocrystalline diamond (UNCD) and mixtures of UNCD with 10%–20% nano-boron-carbide (B_4C) with methane gas at temperatures near 1200 K results in mechanically rigid compacts called nanocarbon ensembles and boron doped nanocarbon ensembles, respectively. It needs to be understood that the amount of boron that enters into a substitutional solid solution in the nanocarbon ensembles as a dopant is only a small fraction of the quantity added initially.[5] Strongly temperature dependent power factors ($PF=\alpha^2\sigma$, where α is the Seebeck coefficient and σ is the electrical conductivity) that increase 30–40-fold between ambient and 1000 K were found for boron doped versus

a)Electronic mail: dmgruen@anl.gov.

undoped material.[4] Here we present recent results aimed at enhancing the thermoelectric performance of these ensembles including materials prepared by reacting methane with boron doped nanographite (NG) starting materials. In the current paper, measurements of PFs have been made up to 1200 K on samples annealed at temperatures up to 2500 K. Anticipating the detailed discussion of the results we note that the PFs continue to increase even at 1200 K, the current limit of our measuring apparatus. For a given temperature, they are more than an order of magnitude larger than for unannealed nanocarbon ensembles due both to increasing Seebeck coefficients and electrical conductivities.

The current work is part of a materials development program based on multicomponent nanoensembles chosen in part for its flexible processing conditions. This approach enables one to exploit advantageously a large parameter space that can be varied over a wide range. An important goal of the research is the discovery of optimization criteria operating in concert on all three quantities entering the expression for the figure of merit of thermoelectric materials. Optimized properties, particularly if they reinforce one another, might be able to overcome to some degree the performance limitations of current thermoelectric materials.

II. EXPERIMENTAL DETAILS

Disperse UNCD (5–10 nm particle size) or NG (30 nm particle size) powders,[6,7] either pristine or mechanically mixed with 5 wt % of nano-B_4C (50 nm particle size),[8] were placed in $20\times10\times5$ mm^3 highly oriented pyrolitic graphite crucibles and treated with methane gas in a quartz vessel heated in several intervals from ambient temperatures to 1200 K in a tube furnace. The contents of the crucibles gained between 70% and 100% in weight with the greatest change occurring between 950 and 1050 K. For UNCD, NG, and their mixtures with B_4C this procedure resulted in the formation of mechanically rigid compacts with densities of 1.5–1.7 g/cm^3. From now on the ensembles containing UNCD will be referred to as NDEs and those containing NG as NGEs. The corresponding samples mixed with B_4C will be labeled as doped NDEs and doped NGEs, respectively. Ensembles heated to 1200 K are called "as-fabricated" samples to distinguish from samples that have been annealed in a mixture of Ar-4%H_2 in a furnace with SiC heating elements to 1700 K and in a carbon furnace in argon to 2500 K for varying lengths of times. Some of the samples experienced a minor weight loss after annealing.

Scanning electron microscopy (SEM) micrographs were obtained using a HITACHI S-4700 field emission gun scanning electron microscope. Raman spectra at an excitation wavelength of 632.8 nm were collected at room temperature, using a Renishaw micro-Raman RM2000 on a 50× objective over the range of 50–4000 cm^{-1} using an ~1 μm spot size. No sample preparation was required as measurements were found to be highly reproducible for different sample areas. X-ray diffraction (XRD) data (Rigaku miniflex +diffractometer with Cu $K\alpha$ radiation ($\lambda=0,154$ nm)) were collected from 3° to 90° 2θ with a scan speed of 2 s/step and a step size of 0.02°. Diffraction patterns were taken of as fabricated and as well as of annealed samples. Phase identification was based on the International Center for Diffraction Data database.

High resolution transmission electron microscopy (HR-TEM) was performed using a field emission FEI Tecnai F20 operating at 200 keV. The transmission electron microscopy (TEM) samples were prepared by scraping the compact bulk samples and dispersing the resulting powders in ethanol. The dispersions were ultrasonicated and subsequently deposited on a holey carbon 3 mm copper grid.

Seebeck coefficients and dc electrical conductivities were measured using an apparatus based on a well-established design.[9] It consists of a 1800 K, single-zone tube (mullite, 4.4 cm inside diameter) furnace and controller, a Keithley 2700 multimeter/data acquisition system, and a Keithley 6220 current source, all controlled by a computer using LABVIEW. The ends of the tube were water cooled and sealed with end caps that allowed fittings for thermocouples and gas inlet/outlet valves.

The alumina sample holder made from a closed-end tube fits into a larger outer tube. One-half of the outer wall was removed about 10 cm from the closed end for access. A spring-loaded alumina push rod was used to hold the sample ($25\times8\times3$ mm^3) against Pt foils placed at each end of the sample. Pt/Pt+10% Rh thermocouples were spot welded to the foils. The thermocouples were used both to measure temperature and to supply 10 mA of current for the conductivity measurements as well as the temperature. Two small notches cut in the sample by a thin (0.175 mm) diamond saw blade at positions about 1/3 and 2/3 from the sample ends served to hold thin, tightly wound (0.075 mm) Pt wires cemented to the sample using Pt ink. These wires secured two additional Pt/Pt+10% Rh thermocouples to measure the voltage generated by the 10 mA current. The data acquisition system recorded the conductivities as well as the six voltages and temperatures generated by the temperature gradient. The gradient could be adjusted by moving the sample holder's position within the furnace. The Seebeck coefficient $\alpha=-\lim_{\Delta T\to0}(\Delta V/\Delta T)$ was calculated from the slope of a plot of ΔV versus ΔT in the limit of $\Delta T=0$. At high temperatures, there was larger scatter in the data. However, α values were considered only if the regression fit parameter $R^2>0.90$. Correction for the voltage arising from the differences in the length of the Pt wires was included. All measurements were performed in flowing argon gas.

III. RESULTS

A. SEM

SEM micrographs for the doped NGE and NDE samples for as fabricated at 1200 K or annealed at higher temperatures [i.e., 2500 K (4 h) for NGE samples and 2100 K (4 h) for NDE samples] are shown in Fig. 1. SEM demonstrated that the original UNCD or NG powders retained their particle shape and size though they agglomerate and are surrounded by carbon deposits that grow as a result of the reaction with methane at temperatures up to 1200 K (Fig. 1). In addition the as-fabricated 5% B_4C-NDE shows the growth of 200–500 nm long rods whose composition and structure

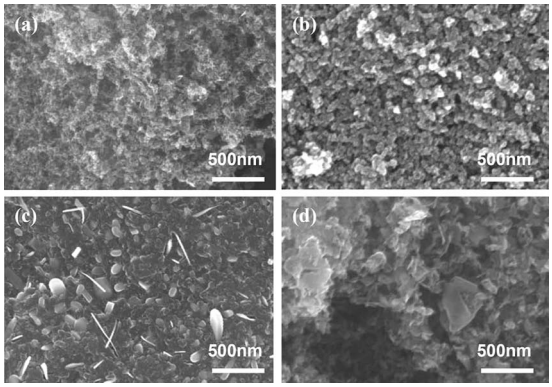

FIG. 1. SEM micrographs: (a) 5% B_4C-NGE samples at 1200 K (as fabricated) and (b) at 2500 K (4 h) and (c) 5% B_4C-NDE samples at 1200 K (as fabricated) and (d) at 2100 K (4 h), respectively.

have not yet been determined. These disappear upon annealing to 2100 K. No further discussion of the SEM micrographs will be given here. The reader is referred to Sec. III D where the structural transformations of sp^2 bonded carbon formed by thermal decomposition of methane are followed as a function of annealing temperature. In that section, mention is also made of the gradual graphitization of the UNCD particles at the higher annealing temperatures.

B. Raman spectroscopy

Raman scattering experiments have been carried out on the ensembles. Defect structures in the nanocarbon components of the ensembles break the hexagonal symmetry of the graphite lattice and modify the optical selection rules for the lattice vibrational modes. A single Raman line, the *G* peak, is theoretically expected for single crystal graphite and is, in fact, observed around 1580 cm^{-1} in natural graphite and stress annealed pyrolitic graphite. An additional Raman line is observed in the range 1330–1360 cm^{-1} in glassy carbon, polycrystalline graphite or diamondlike carbon. This well known *D* peak, which also relates to graphitic sp^2-bonding, is associated with structural disordering and its position is known to change with excitation wavelength. The *D* peak is said to arise from graphite containing disorganized regions near crystal edges and lattice defects (i.e., dislocations, vacancies, and interstitial carbon atoms between the basal planes of carbon atoms).[10]

The Raman spectra of the 5% B_4C-NGE (left) and 5% B_4C-NDE (right) samples prepared under various conditions are shown in Fig. 2. The Raman scattering spectra, typical of high temperature carbon nanostructured materials under red laser excitation, reveal the above mentioned peaks at around 1330 and 1595 cm^{-1}, which are assigned to the disorder-induced and E_{2g} modes of graphite, respectively. Similar spectra have been obtained reproducibly for different series of samples.

The D/G intensity peak ratio, extrapolated from the spectra after fitting of the data with a Gaussian function and subtraction of the baseline for each spectrum, is related to the cluster size or in-plane correlation length (L_a).[10,11] An increasing value of their quantity implies an increase in the clustering or number of aromatic rings per clusters. The D/G intensity peak ratio varies from 1.35 at 1200 K to 1.52 at 2500 K/4 h for the 5% B_4C-NGEs and from 1.5 at 1200 K to 1.75 at 2100 K for the 5% B_4C-NDEs. Similar trends have been observed for the samples heated at 1700 K for various times. An analysis of our data gives values for L_a in the range 21–24 nm for the NGE samples and 24–28 nm for the NDE samples, correlating with the structural modifications of the materials as a result of the annealing process and consistent with the results of the TEM measurements, as will be shown later.

C. XRD

Our XRD investigations were directed primarily to changes in shape and width of the graphite diffraction peaks and the transformation of diamond to graphite as a function of temperature. Generally speaking, graphite peak intensity increased and peak width decreased with annealing temperatures above 1500 K. The influence of the heat treatment upon graphite interlayer spacing is illustrated in Fig. 3. Typical XRD data on carbon ensembles representative of doped

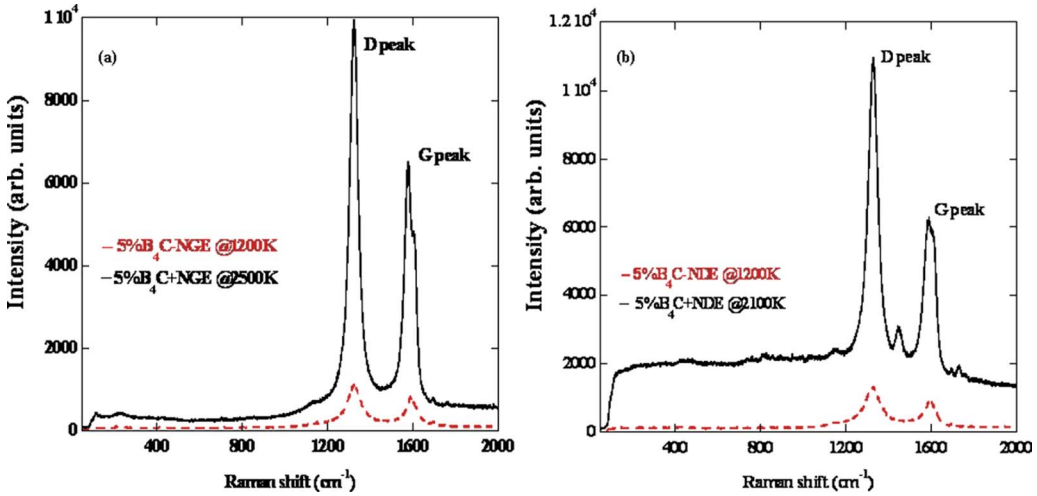

FIG. 2. (Color online) Raman spectra corresponding to (from left to right) (a) 5% B_4C-NGE samples at 1200 K (as fabricated) and after annealing at 2500 K for 4 h and (b) 5% B_4C-NDE samples at 1200 K (as fabricated) and after annealing at 2100 K for 4 h.

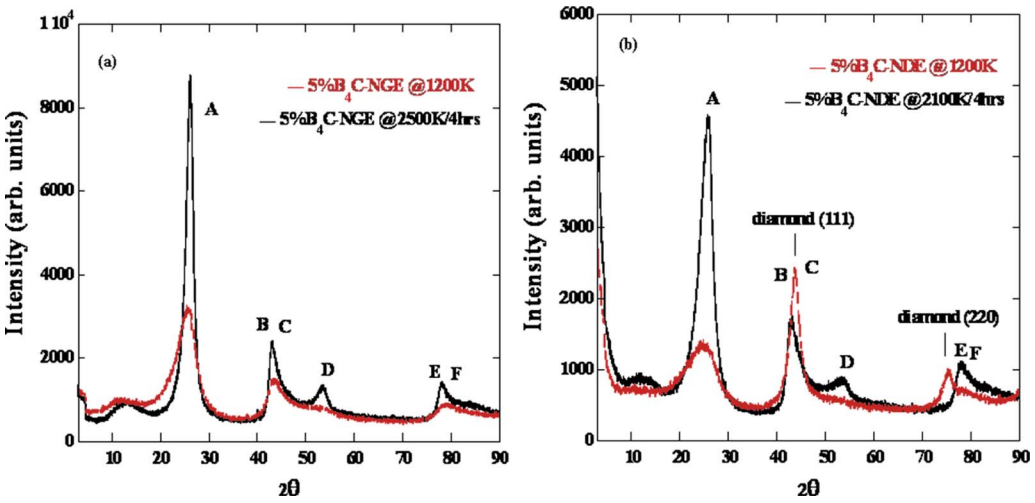

FIG. 3. (Color online) XRD spectra corresponding to (from left to right) (a) 5% B_4C-NGE at 1200 K (as fabricated) and after annealing at 2500 K for 4 h and (b) 5% B_4C-NDE samples at 1200 K (as fabricated) and after annealing at 2100 K for 4 h. A, B, C, D, E, and F are graphite diffraction peaks indexed to (002), (100), (101), (004), (110), and (112), respectively. Diamond reflections, (111) and (220), are also pointed out in the figure on the right.

NGEs (left) and NDEs (right) are presented. The NGEs show peaks at the graphite (002), (100), (101), (004), (110), and (112) positions. The NDEs have additional peaks corresponding to the diamond (111) peak located near 45° where graphite (110) and (112) peaks merge into a single broad peak and the diamond reflection (220) near 78°.

As shown in Fig. 3 annealing the samples in an argon atmosphere results in a slight shift of the position and sharpening of the Bragg peaks. Knowledge of both the position and the full width at half height of the diffraction peaks as a function of the annealing temperature and times allows one in principle to monitor the evolution of the nature of the phases as a function of temperature with graphite materials that are prone to Hendricks–Teller layer disorder.[12] One cannot calculate the crystallite size or internal strain effects but one can follow the evolution of the interlayer (002) distance. The d_{002}-spacing can be obtained by measuring the 2θ angle at the maximum of the 002 peak of graphite and use its value in the Bragg equation to get the mean d_{002}-spacing of the sample: $2\theta_{hkl}\sin(\theta_{hkl})=n\lambda$, where $2\theta_{hkl}$ is the scattering angle and d_{hkl} is the spacing between the hkl planes. As a result of this analysis for all the series of nanocarbon ensemble samples, we note that the distance decreases from 0.344 nm for 5% B_4C containing NGE as-fabricated samples at 1200 K to 0.334 nm after a 12 h anneal at 1700 K and from 0.351 to 0.337 nm for the 5% B_4C-NDE samples for the same set of annealing conditions (versus 0.336 nm for graphite, ICDD: 37-0798).

The evolution of the d_{002}-spacing with annealing provides an approach in understanding the graphitization behavior. Although the d_{002}-spacing does not give quantitative data on the degree of graphitization, measuring the change in spacing remains a convenient way to compare relative degrees of graphitization within materials of the same family. The width of the [002] peak was demonstrated to be a good qualitative measurement of the unorganized carbon content in carbonaceous materials.[13] On this basis, the observed decreases in d_{002} values between annealed and as-fabricated samples imply that the thermal treatment reduces the amount of unorganized (disordered) carbon, as expected.

D. HRTEM

The TEM study reported in this work examines the morphology, the composition, and the structural transformations of the nanocarbon ensembles resulting from different annealing treatments. These studies are designed to give detailed information on changes in nanocarbon structures as a function of annealing temperatures and to correlate these structures insofar as possible with changes in thermoelectric properties.

Prior to heating and reaction with methane the original NG particles had a spherical shape and a size of between 15 and 30 nm characteristic of poorly crystallized NG. In order to follow the structural transformations that occur as a result of annealing, we take advantage of the fact that the HRTEM imaging mode gives access to the atomic scale crystallographic structure of a material. Figures 4(a)–4(c) show a set of TEM micrographs acquired on different as-fabricated NGE samples prepared at 1200 K. They consist of a mixture of sp^2 carbons forming agglomerates. Figure 4(a) corresponds to a high magnification micrograph of one of these agglomerates which consist of randomly distributed porous curved surfaces. The size and the shape of the nanopore structures indicate a transformation from the original nanographitic particles. It is important to note that these NGEs are composed of crumpled sets of a few layers of graphene (FLG) sheet, as shown in Fig. 4(b). These FLG structures are more clearly revealed in Fig. 4(c) and seen to consist of less than 20 graphene sheets. Such sheets can be observed in all samples formed from mixtures of nanographitic and boron carbide powders. After reaction with methane the FLG structures persist even after a wide variety of annealing treatments described in more detail below.

It is noteworthy that such structures are not observed in NDEs. Furthermore we have also identified in NGEs, in addition to FLGs, several other nanocarbon constituents: nano-

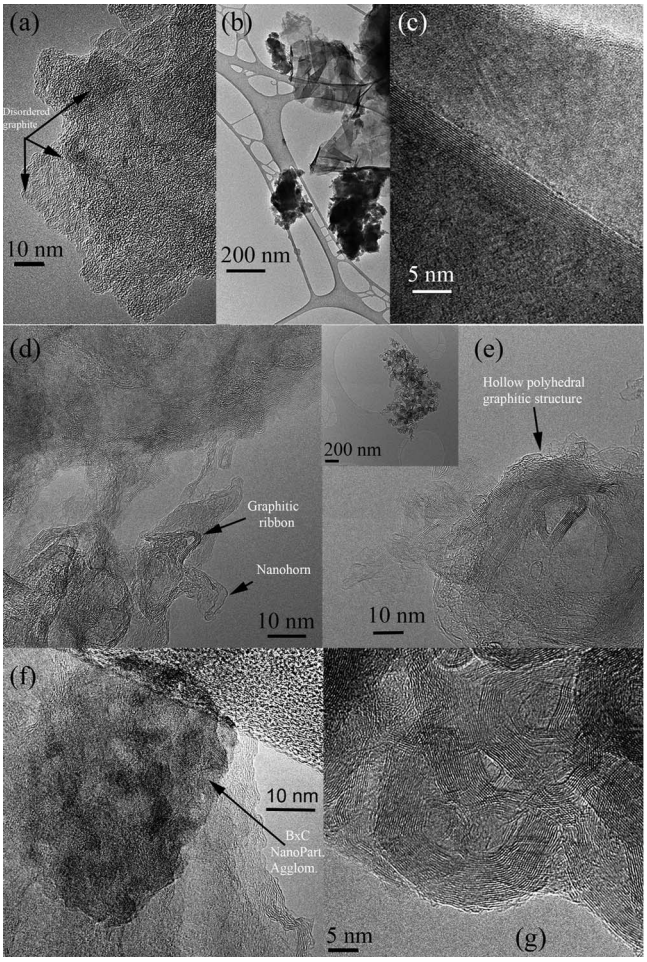

FIG. 4. TEM micrographs corresponding to (a) as-fabricated B_4C doped NGEs, (b) low magnification TEM micrograph of an area showing FLG structures, (c) HRTEM of one of these FLG structures where several sheets of graphene can be discerned, [(d) and (e)] nanocarbon ensemble materials after annealing at 1700 K for 8 and 12 h, respectively, (f) B_xC nanoparticle agglomerate and graphitic curved surfaces, and (g) area showing polyhedrical nanopore structures acquired in a NCE sample after annealing at 2100 K for 4 h.

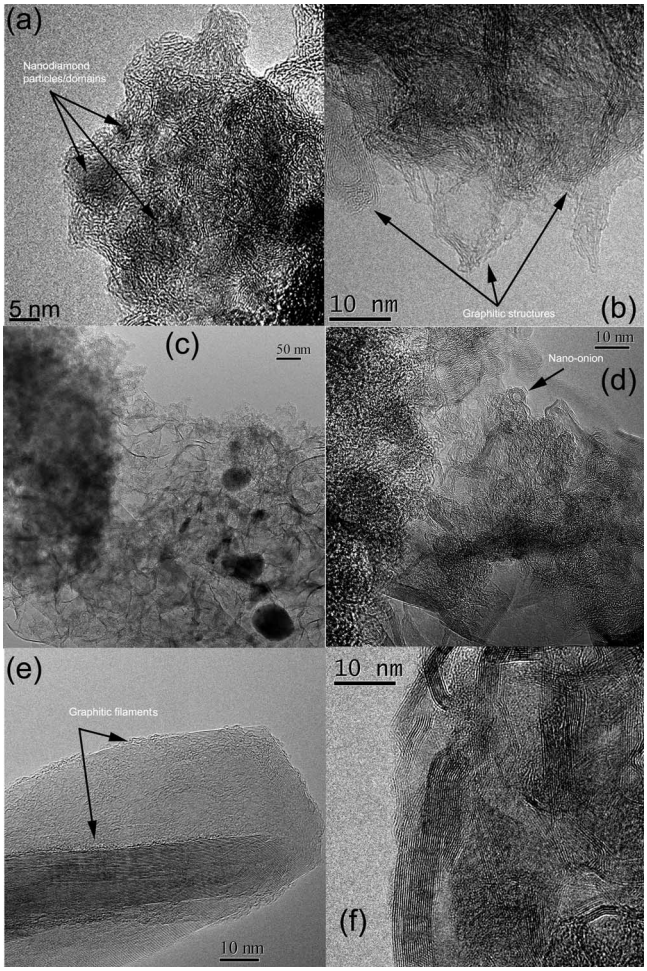

FIG. 5. TEM micrographs corresponding to [(a) and (b)] HRTEM images of as-fabricated B_4C NDEs, showing a mixture of sp^2 and sp^3 bounded carbons (a) and only sp^2 bounded carbon structures (b). (c) and (d) correspond to NDE materials after annealing at 1700 K for 12 h and (e) during 16 h, respectively. (f) Area displaying the nanopore structures formed after annealing at 2500 K for 4 h.

horns, deformed nano-onions, isolated fullerenes, and hollow polyhedral structures.[14] Figure 4(f) shows that boron carbide (B_xC) particles surrounded by a few graphitic layers are also present. Their lattice spacing (0.282 nm) is consistent with the (123) interplanar distance of rhombohedral boron carbide. Annealing at 1700 K leads to an increase in graphitization. The wide variety of curved graphitic surfaces produced under these conditions becomes even more evident when one extends the heating period from 8 to 12 h at 1700 K, Figs. 4(d) and 4(e). After annealing at 2100 K for 4 h, the degree of graphitization of the NGEs is even more pronounced [Fig. 4(g)], as evidenced by an area containing hollow polyhedral structures.

We turn now to describe the as-fabricated B_4C doped NDEs prepared at 1200 K. These NDEs consist of a mixture of sp^2 and sp^3 bonded carbons [Figs. 5(a) and 5(b)]. It can be seen that the effect of the reaction with methane transforms the original UNCD constituted of 5–8 nm particles to particles surrounded by several kinds of sp^2 bonded carbons [Fig. 5(b)]. Annealing of the as-fabricated NDEs at 1700 K for 12 h induces graphitization of the UNCD particles. This process becomes more pronounced as the annealing time is increased from 12 to 16 h, Figs. 5(d)–5(f). After the longer annealing time, the UNCD content is reduced and is replaced by a complex mixture of nanocarbon filaments, needles, and cones [Fig. 5(e)]. Annealing at 2500 K for 4 h completely transforms the original NDE's as-fabricated material. The amount of sp^3 bonded carbon is significantly reduced and replaced by agglomerates of nanoporous structures, showing graphitic curved surfaces, see Fig. 5(f).

E. TE measurements

Seebeck coefficient (α) and dc electrical conductivity (σ) were measured for doped and undoped NGE's and NDE's as fabricated and after various annealing temperatures for 4, 8, and 12 cumulative anneal times. Furthermore doped and undoped NGEs and NDEs were measured after annealing for 4 h at 2500 and 2100 K, respectively. Thermopower measurements at temperatures up to 1200 K were made.

Figures 6(a) and 6(b) show that the Seebeck coefficients measured as a function of temperature for the 5% B_4C-NGEs

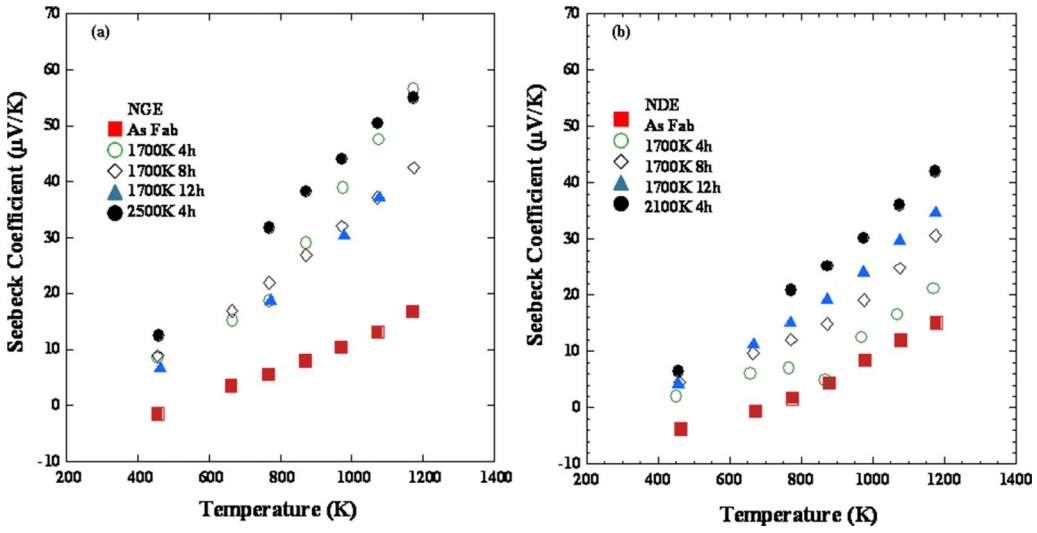

FIG. 6. (Color online) Seebeck coefficients of (a) 5% B_4C-NGEs and (b) 5% B_4C-NDEs as a function of temperature and annealing times.

and 5% B_4C-NDEs for various annealing temperatures and times were found to increase monotonically with measuring temperature in both sets of samples. There is a pronounced increase in the magnitude of the Seebeck coefficient for the annealed as compared to the as-fabricated samples.

For the 5% B_4C-NGE samples, the Seebeck coefficient depends to a considerable extent on the annealing time. Annealing at 2500 K for 4 h showed similar values as the 4 h 1700 K anneal. It should be noted that data for as-fabricated and 1700 K anneal were for the same sample, whereas the 2500 K annealing was conducted on a different sample fabricated under identical conditions.

Seebeck behavior for the 5% B_4C-NDEs was similar to the 5% B_4C-NGEs. Annealing temperature and times showed enhancement in the Seebeck coefficients at all temperatures of measurement. A general trend of increasing Seebeck coefficient with the temperature was observed for all samples. There seems to be a systematic increase in α with annealing time for the NDEs. However, it appears that the magnitude of the Seebeck coefficient is somewhat smaller than those observed for the 5% B_4C-NGEs. Here again, data for as-fabricated and 1700 K annealing were from the same sample, and 2100 K anneal test was conducted on a different sample.

Figures 7(a) and 7(b) show the dc electrical conductivity for 5% B_4C-NGEs and 5% B_4C-NDEs. The as-fabricated NGEs exhibited about two times higher conductivity compared to NDEs. With annealing at 1700 K for various times, the increase in electrical conductivity was much larger for the NDE samples. Also, the magnitudes for both NGE and NDE samples were similar to values of approximately 150 S/cm. After >2100 K annealing treatment, both sets of samples showed significant increases in room temperature electrical conductivity with values of 350 and 280 S/cm for the NGE and NDE samples, respectively. As a function of temperature, NGEs showed somewhat decreasing values while for the NDEs the conductivity appears to increase slightly with temperature and to saturate at 300 S/cm.

PFs ($\alpha^2\sigma$) for 5% B_4C containing NGEs and NDEs were calculated and plotted in Figs. 8(a) and 8(b). It can be seen that annealing dramatically increases the PF by as much as an order of magnitude. The 2500 K anneal showed the high-

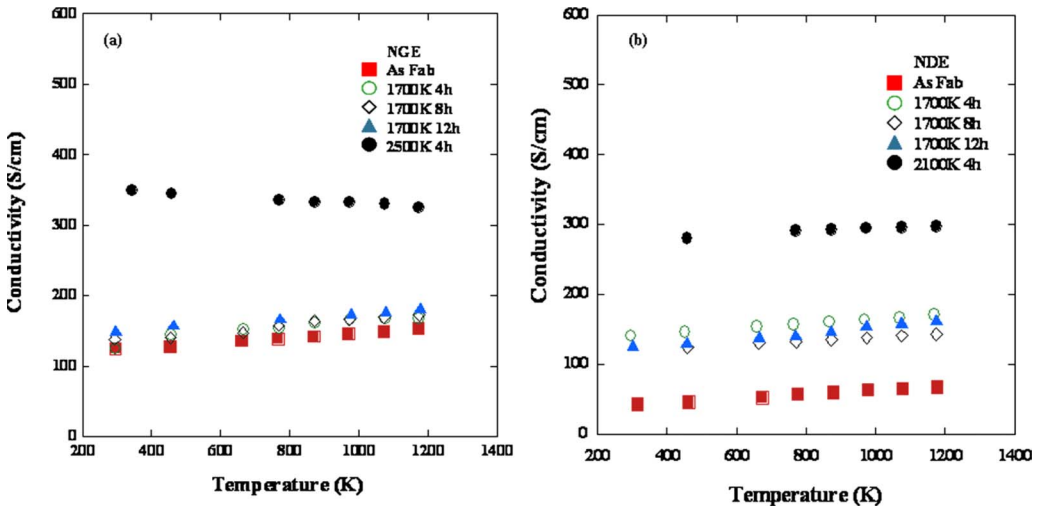

FIG. 7. (Color online) dc electrical conductivity (a) 5% B_4C-NGEs and (b) 5% B_4C-NDEs as a function of temperature and annealing times.

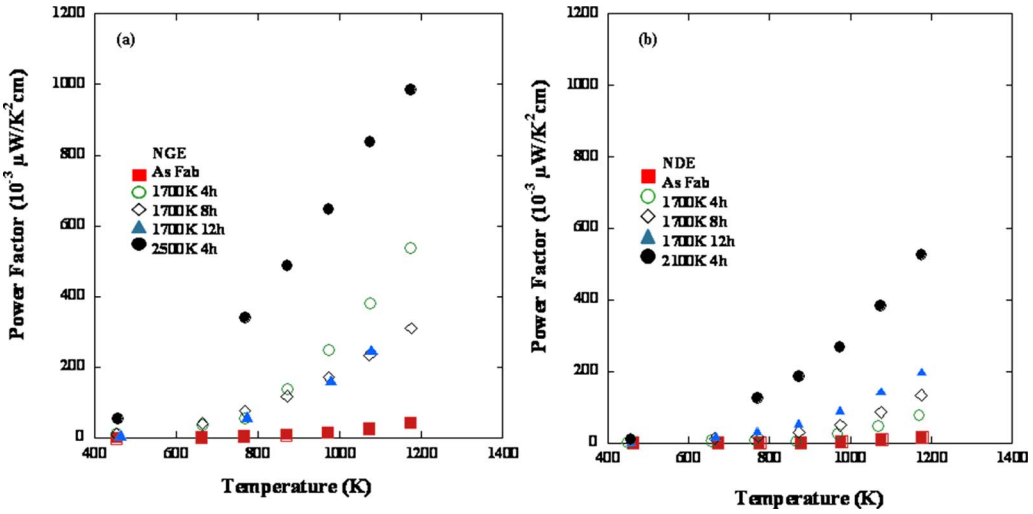

FIG. 8. (Color online) PFs of (a) 5% B_4C-NGEs and (b) 5% B_4C-NDEs as a function of annealing temperature and times.

est PF in part because of the dramatic increase in electrical conductivity. With our measuring system, we are limited to reliable Seebeck and electrical conductivity measurements up to 1200 K.

Figure 9 shows the PFs for the undoped NGE sample measured as a function of temperature for the as-fabricated sample and after annealing for 4 h at 1700 K. Comparing Figs. 8(a) and 9 gives insight into the role of boron additions. For both boron doped and undoped samples, as-fabricated PFs are almost identical as a function of temperature. However, the effect of boron additions becomes very apparent after annealing of the samples. The PFs are enhanced by at least a factor of 3 when B_4C is added to the NG or nanodiamond powders before reaction with methane.

IV. DISCUSSION

The approach to the development of more efficient thermoelectric materials underlying the present work is based on the idea that bulk readily available, nontoxic, relatively inexpensive nanostructured materials that resist recrystallization could limit detrimental electrical and thermal losses while using straightforward fabrication routes. It was recognized at the outset that one of the challenges that must be overcome by such an approach is electron scattering at interfaces between randomly oriented grains leading to a concurrent reduction in both the electrical and thermal conductivities.[1] The most thoroughly studied system exemplifying this approach appears to be that based on boron doped silicon-germanium where recent work suggests that nanostructured SiGe does, in fact, enhance *ZT*.[2] However, it appears to us that a systematic study of the degree to which thermopower as well as electrical and thermal conductivities can be independently controlled and optimized taking advantage of structural and compositional variations in intimately mixed nanocomposite structures has not been carried out on a model system. We have chosen nanocarbon ensembles as a model system because of its suitability with regard both to its physicochemical properties and because it lends itself to a rigorous and detailed quantum-mechanical theoretical treatment.

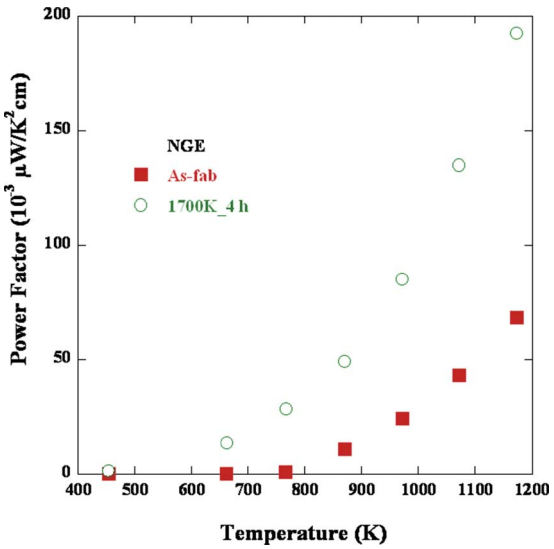

FIG. 9. (Color online) PFs as a function of temperature of NGEs for various temperatures for the as-fabricated sample and after annealing for 4 h at 1700 K.

The initial results presented here confirm that the nanocarbon ensembles fulfill the requirements of a model system in both regards. For example, substantial PFs of 1 $\mu W/K^2$ cm have already been reached with boron doped NG ensembles after anneals at 2500 K (Figs. 6–8). The very substantial increase in PF over earlier work carried out at 1200 K (Ref. 4) is believed to be primarily due to the high annealing temperatures which lead to higher boron doping levels and thus to higher Seebeck coefficients as well as to nanostructural changes that result in a doubling and tripling of the electrical conductivity. Preliminary measurements have shown that the thermal conductivities of the nanoensembles are in the range 0.03–0.07 W/cm K.[15] Taken together, these results which will be discussed in detail below indicate that the nanocarbon ensembles have considerable promise as thermoelectric materials. Clearly, however, marked improvement in their performance is required in order for them to function as efficient energy convertors. To

reach that goal, future generations of ensembles must display substantial increases in thermopower, for example, without a concomitant decrease in their electrical or increase in their thermal conductivities.

A rational approach to the solution of this extremely challenging problem will depend on how successfully one can establish an interplay between experimental approaches while at the same time achieving a better theoretical understanding of the factors determining transport in these materials. A particularly difficult aspect concerning thermoelectric phenomena has been the question of electronic entropy transport in a thermal gradient which determines the magnitude and temperature dependence of the Seebeck coefficient. The nanocarbon ensembles offer an interesting opportunity to make progress in this difficult area. It has been known for a long time that boron doping induces an acceptorlike feature near the top of the valence band of graphitic substances.[16,17] However, the crucial role in determining thermoelectric properties played by the unique nature of the graphite lattice in providing a multitude of boron substitutional configurations each with its distinctive energy signature appears to have been explicitly recognized for the first time in our earlier work.[4] This recognition led us to examine in detail the nature of the acceptorlike feature using density functional calculations on boron substituted polyaromatics that serve as molecular models for finite as well as stacked graphene sheets.[18] These calculations provide insight into the relative stabilities of high spin versus low spin states as a function of graphene sheet size, Kekule versus non-Kekule structures, as well as the effects on orbital energetics of various boron substitutional configurations.

Insights emerging from this theoretical work provide detailed understanding of the many thousands of possible boron geometric configurations each one associated with a distinct "molecular analog" electronic state. Our calculations predict a lowering of the Fermi level by about 0.1 eV due to boron doping, thus creating a vast number of empty, perhaps nearly degenerate states that can be populated thermally leading to a situation that could foster an augmentation of electronic entropy. This cluster approach in exploring the electronic structure of boron doped nanocarbons can hopefully be extended to help establish a better understanding of the factors determining the magnitudes and temperature dependencies of the decisive entropic flows that determine the ergodic processes accompanying hole as well as electron transport in thermal gradients A deep understanding of the complex issues underlying these phenomena is clearly a first step in the fashioning of more efficient heat to electricity conversion materials.

The interplay between experimental and theoretical results in establishing the nanocarbon ensembles as model systems to help in understanding the factors underlying thermoelectric behavior in a more general sense will be clarified in the following discussion. The extensive and highly reproducible thermoelectric measurements made on several sets of samples leave no doubt that both annealing temperatures and annealing times profoundly affect the magnitude and temperature dependencies of the Seebeck coefficients and the electrical conductivities. The effects of annealing profiles on boron doped ensembles, however, are different for NGEs and NDEs, as is evident from an examination of Figs. 6(a) and 6(b). The dramatic effects of boron concentration, [B], on both the magnitude and the temperature dependence of the Seebeck coefficient, α, are illustrated in Figs. 6(a) and 6(b). If α were linearly dependent on [B] one would expect that quantity to increase by at least two orders of magnitude in going from 1200 to 2500 K anneals based on the boron solubility data of Lowell[5] who determined the solubility of boron in graphite as a function of temperature. The smaller than expected observed factor of 5 increase in α for measurements made at 1200 K probably reflects boron partially coming out of solid solution to reform B_4C as the NG ensemble slowly cools over a period of hours in the large resistance heated graphite furnace. This interpretation gathers support from data taken on a nanodiamond ensemble after a 2100 K anneal in the same furnace which displays an α value intermediate between 2500 and 1700 K anneals. An accurate determination of the functional relationship between α and [B] will require the development of a procedure that allows doping to be done in a controlled way and we are exploring paths to accomplish to this end.

Boron is known to be a dopant both for diamond and for graphite.[19,20] The difference in behavior of α between NGEs and NDEs is probably due to a difference in the effect of boron on the thermoelectric properties of these two allotropes of carbon. Here we wish merely to point out that continued annealing up to 12 h of NDEs at 1700 K gives α values that increase with heating time approaching those observed with NGEs [compare Figs. 6(b) and 6(a)]. XRD measurements show that nanodiamond slowly converts to NG at these temperatures and we believe that the observed increase in α is traceable to this circumstance. This question will be considered in more detail after a discussion of the electrical conductivity and PF results.

The difference in behavior of the electrical conductivity (σ) between NGEs and NDEs displayed graphically in Figs. 7(a) and 7(b) is due to two important considerations. In the NGEs, the nanocarbon constituent is entirely NG except for the presence of 5% B_4C. The σ for the 1200 K as-fabricated samples are not changed much after annealing at 1700 K. However, at 2500 K, a large increase in σ by a factor of 2 or 3 is observed which we attribute to a major structural ordering of the NG component. This important reorganization phenomenon has been followed in detail by HRTEM and XRD. By comparison, a marked increase in σ is observed in the NDEs when the 1200 K as-fabricated samples are annealed at 1700 K because the major original nanodiamond component slowly converts to NG at this temperature. Interestingly, the σ of NDEs annealed at 2100 K are quite similar to those of NGEs annealed at 2500 K, indicating that conversion of diamond to graphite may be virtually complete at 2100 K.

The PFs ($\alpha^2\sigma$) for the NGE and NDE compacts are shown in Figs. 8(a) and 8(b). For both sets of samples, the PFs increase strongly with temperature and continue to do so even at 1200 K, the upper limit of our thermoelectric measurements, with no indication of reaching a plateau. Significantly, a value of 1 $\mu W/K^2$ cm is attained with NGE com-

pacts annealed at 2500 K. Preliminary measurements of the thermal conductivity of the compacts have been carried out[15] and give values in the range $(3-7)\times10^{-2}$ W/cm K. Figures of merit calculated using PF and thermal conductivity values on the current generation of samples are too low to be of interest for applications. Considerable improvement in the performance of the nanocarbon ensembles is required and efforts in this direction are underway.

As already stated in Sec. III, prior to heating and reaction with methane, the original NG particles in the NGEs had a spherical shape and a size of between 15 and 30 nm. They are formed of a poorly crystallized graphite structure. Reaction with methane at 1200 K produces a 70%–100% weight gain due to the growth of intergranular carbon that strongly bonds the loosely agglomerated NG particles into mechanically rigid compacts. Although the detailed mechanism of this process has not been elucidated, certain aspects of the reaction leading to the transformation can be understood on the basis of HRTEM data. Crumpled sheets of graphene [Figs. 4(b) and 4(c)] are formed at 1200 K as well as a complex mixture of nanohorns, deformed nano-onions, fullerenes, and hollow polyhedral nanostructures. The annealing at 1700 K increases the graphitization of these materials. Finally, annealing at 2100 K produces a reduction in the number of crystalline defects concomitant with an increase in the degree of ordering due to higher stacking perfection of carbon layers.

The nanostructural changes due to annealing shown by HRTEM are also reflected in the XRD data [Fig. 3(a)] which can be indexed to graphite reflections as follows: near 25° (002), near 45° (100) and (101), and near 80° (110) and (112). Annealing to 2500 K causes the expected narrowing of the (002) peak that is known to accompany an increase in the ordering of the graphitic planes. The small shift of that peak to larger values of theta is generally attributed to a decrease in the interplanar distance, in our case from 0.344 to 0.334 nm following extensive "graphitization" associated with the ordering of layers.

The magnitude of σ suggests that one is dealing with hopping conductivity[21] characteristic of disordered materials with a local disordering length of a few interatomic distances. A qualitative description of the conductivity changes observed in the nanocarbon ensembles can be given on the basis of Mott's concept of hopping conductivity.[22] At annealing temperatures up to 1700 K conductivity occurs primarily along carbon chains and defected planes. At higher temperatures, graphene sheets, fullerenic structures, and other curved surfaces provide better conduction paths. Finally at the highest annealing temperatures employed in the present work, 2500 K, the formation of hollow polyhedral NG structures with reduced numbers of defects provides excellent conduction paths leading to σ values of 300 S/cm and above. Clearly, a more detailed understanding of conductivity in these materials will require both extensive experimental measurements, for example, of the temperature dependence and the Hall coefficients as well as a thorough theoretical treatment of electronic transport in these nanoporous materials.

From a theoretical point of view, the main features of the TE performance of the NGEs have been shown in recent density functional calculations to arise from changes in the electronic structure of NG as a result of boron doping.[18] These cluster or molecular analog calculations can be usefully compared to results from a simple two band model elaborated to explain the performance of boron doped bulk graphite thermocouples.[20] As already discussed, the dramatic effects of annealing on the magnitude of α and σ can be qualitatively understood on the basis of an increased solubility of boron in graphite with temperature on the one hand and more favorable conduction paths arising from highly ordered and less defective graphite layers on the other hand.

The results on the NDEs [Figs. 6–8] are interesting particularly from the point of view of the light they shed on the transformation of UNCD to NG as a function of temperature. Of particular importance for the present study is the work of Kuznetsov and and Butenko[21] and Kuznetsov *et al.*[23] as well as that of Andersson *et al.*[17] This by now quite well developed subject will be discussed here only to the extent that it relates to NDE thermoelectric properties. Annealing affects α and σ not only because of changes in boron solubility and ordering of graphene structures but also because of the transformation of UNCD to NG. In the as-fabricated NDE, UNCD is the primary constituent prior to reaction with methane. The UNCD to NG transformation has been followed in our work using XRD, HRTEM, and Raman characterization techniques. An exemplar of the XRD data is shown in Fig. 3(b). The diamond (111) reflection is at a somewhat smaller 2θ angle than the graphite (100) and (101) reflections and overlaps the latter two reflections, thus making it difficult to use this Bragg region to follow the transformation quantitatively. Our data analysis is therefore based on a determination of the ratios of intensities of the diamond (002) near 75° relative to the graphite reflections near 80°. In this Bragg region, the diamond and graphite reflections are reasonably well resolved. The detailed work of Andersson *et al.*[17] provides us with baseline information regarding the temperature dependent transformation of disperse UNCD to graphite. Their data and ours are in excellent agreement.

The HRTEM micrographs (see Figs. 4 and 5) substantiate the conclusions reached on the basis of the XRD measurements. As an example, NDEs annealed at 2100 K show a greatly diminished number of UNCD crystallites compared to the as-fabricated compacts with only a few 2–5 nm UNCD particles remaining at that temperature. Structures displaying graphitic and curved surfaces abound with equidistant sheets forming essentially defect free layers.

V. CONCLUSIONS

Thermoelectric PFs of nanocarbon ensembles have been determined as a function of temperature from 400 to 1200 K. The ensembles are composed of (a) mixtures of NG and 5% B_4C called NGEs or (b) mixtures of UNCD disperse powders and 5% B_4C called NDEs. The mixtures are formed into mechanically rigid compacts by reaction with methane gas at temperatures up to 1200 K. They are then annealed at various temperatures and various lengths of time up to 2500 K.

Boron substitutional doping occurs primarily during the annealing steps up to maximum concentrations estimated to be about 1%.

The ensembles were characterized using SEM, Raman scattering, XRD, and HRTEM techniques to gain insight into the structural changes attending high temperature treatment of the nanocarbons. The compacts retain their nanostructural characteristics up to the highest annealing temperatures but display complex structural transformations going in the case of NGEs from turbostratic NG to a complex mixture of fullerenes, nano-onions, and nanotubes to hollow nanopolyhedra as the temperature is increased. For NDEs, the temperature at which UNCD transforms to NG overlaps the temperature regime where a variety of NGs evolve with increasing temperature and annealing time. Our results on UNCD graphitization are in agreement with detailed literature studies on this topic.

The thermoelectric PFs of the ensembles increase strongly both as a function of annealing temperature and of the temperature at which the measurements are carried out. They reach values of 1 $\mu W/K^2$ cm at a 1200 K measuring temperature for samples annealed at 2500 K. Seebeck coefficients of 60 $\mu V/K$ and electrical conductivities of near 350 S/cm have been measured. Preliminary results of thermal conductivity are in the range 0.03–0.07 W/cm K. Figures of merit based on these measurements are too low to be of practical interest. We conclude that the most promising next step for improved performance is to attempt to raise the values of the Seebeck coefficient.

Detailed density functional calculations of molecular analog model systems[18] have shown that boron substituting for carbon on graphite lattice sites leads to a lowering of the Fermi level and the creation of a large number of empty states within thermal excitation energies of the Fermi level. We attribute the magnitude and temperature dependence of the thermoelectric PFs to the enhancement of electronic configurational entropy resulting from the boron "doping" of the nanocarbons that comprise the ensembles.

ACKNOLEDGEMENTS

This work was performed under the auspices of the U.S. Department of Energy, Office of Basic Energy Science and Energy Efficiency Renewable Energy, Office of Vehicle Technologies, under Contract No. DE-AC02-06CH11357 at Argonne National Laboratory, managed by the University of Chicago, LLC. The authors are grateful to Dr. Hsin Wang and Dr. Wallace Porter at the High-Temperature Material Laboratory at ORNL for measuring the thermal conductivity and to Dr. Eric J. Wuchina at the Naval Surface Warface Center for the anneals at temperatures higher than 1700 K. Furthermore, they acknowledge ANL's Electron Microscopy Center for the use of their facilities.

[1] G. J. Snyder and E. S. Toberer, Nature Mater. **7**, 105 (2008).
[2] M S. Dresselhaus, G. Chen, M. Y. Tang, H. Lee, D. Z. Wang, Z. F. Ren, J. P. Fleurial, and P. Gogna, Adv. Mater. (Weinheim, Ger.) **19**, 1043 (2007).
[3] G. A. Slack, in *CRC Handbook of Thermoelectrics*, edited by M. Rowe (CRC, Boca Raton, FL, 1995), pp. 407–440.
[4] D. M. Gruen, P. Bruno, and M. Xie, Appl. Phys. Lett. **92**, 143118 (2008).
[5] C. E. Lowell, J. Am. Ceram. Soc. **50**, 142 (1967).
[6] Obtained from ITC Corporation, Raleigh, NC, http://www.itc-inc.org/nanodiamond2.html.
[7] Obtained from MTI Corporation, Richmond, CA, http://www.mtixtl.com/.
[8] Obtained from American Elements, Merelex Corporation, Los Angeles, CA, http://www.americanelements.com/.
[9] B.-S. Hong, S. J. Ford, and T. O. Mason, Key Eng. Mater. **125–126**, 163 (1997).
[10] A. C. Ferrari and J. Robertson, Phys. Rev. B **64**, 075414 (2001).
[11] R. Arenal, G. Montagnac, P. Bruno, and D. M. Gruen, Phys. Rev. B **76**, 245316 (2007).
[12] P. A. Heiney, M. E. Huster, V. B. Cajipe, and J. E. Fischer, Synth. Met. **12**, 21 (1985).
[13] J. R. Dahn, A. K. Sleigh, H. Shi, J. N. Reimers, Q. Zong, and B. M. Way, Electrochim. Acta **38**, 1179 (1993).
[14] R. Arenal, O. Stephan, P. Bruno, and D. M.Gruen, Appl. Phys. Lett. **94**, 111905 (2009).
[15] Measurements of thermal conductivity and confirmation of Seebeck coefficient made at ORNL.
[16] D. L. Carroll, Ph. Redlich, X. Blase, J.-C. Charlier, S. Curran, P. M. Ajayan, S. Roth, and M. Rühle, Phys. Rev. Lett. **81**, 2332 (1998).
[17] O. E. Andersson, B. L. V. Prasad, H. Sato, T. Enoki, Y. Hishiyama, Y. Kaburagi, M. Yoshikawa, and S. Bandow, Phys. Rev. B **58**, 16387 (1998).
[18] P. C. Redfern, D. M. Gruen, and L. A. Curtiss, Chem. Phys. Lett. **471**, 264 (2009).
[19] A. Balducci, M. Marinelli, M. E. Morgada, G. Pucella, G. Rodriguez, M. Scoccia, and G. Verona-Rinati, Microsyst. Technol. **12**, 365 (2006).
[20] C. A. Klein, in *Chemistry and Physics of Carbon*, edited by P. L. Walker (Dekker, New York, 1966), Vol. 2, p. 225.
[21] V. L. Kuznetsov and Y. V. Butenko, in *Ultrananocrystalline Diamond*, edited by O. A. Shenderova and D. M. Gruen (William Andrew, Norwich, NY, 2006), p. 405.
[22] N. Mott, *Conduction in Non-Crystalline Materials*, 2nd ed. (Oxford Science, New York, 1993).
[23] V. L. Kuznetsov, Y. V. Butenko, A. L. Chuvilin, A. I. Romanenko, and A. V. Okotrub, Chem. Phys. Lett. **336**, 397 (2001).